

# Wind Fragility for Honeycomb Roof Cladding Panels Using Screw Pull-Out Capacity

Viriyavudh Sim, Woo Young Jung

**Abstract**—The failure of roof cladding mostly occurs due to the failing of the connection between claddings and purlins, which is the pull-out of the screw connecting the two parts when the pull-out load, i.e. typhoon, is higher than the resistance of the connection screw. As typhoon disasters in Korea are constantly on the rise, probability risk assessment (PRA) has become a vital tool to evaluate the performance of civil structures. In this study, we attempted to determine the fragility of roof cladding with the screw connection. Experimental study was performed to evaluate the pull-out resistance of screw joints between honeycomb panels and back frames. Subsequently, by means of Monte Carlo Simulation method, probability of failure for these types of roof cladding was determined. The results that the failure of roof cladding depends on their location on the roof, for example, the edge most panel has the highest probability of failure.

**Keywords**—Monte Carlo Simulation, roof cladding, screw pull-out strength, wind fragility.

## I. INTRODUCTION

SMALL-SCALE steel frame residential building whose stories are fewer than two or less than 500 square meters accounted for about 55% of existing buildings in South Korea. In general, steel frame structure composes of the upper steel frame and the base foundation. The superstructure connected to the foundation by connection that can have different arrangement. Thus, the type and configuration of the connection are the main factors to determine the strength and ductility of steel frames [1]. They are sporadically exposed to an extreme wind force, especially during wind disaster, i.e. typhoon. Furthermore, per the Korean Typhoon White Book from Korean National Typhoon Center [2], typhoon disaster in Korea in recent year has been on the rise. The dangers posed by a typhoon can result in devastating losses of economic and human life. Wind loads risk assessment is required to evaluate the design of these structures. Moreover, it has been extensively documented for Probabilistic Risk Assessment (PRA) to be an effective framework to evaluate risk associated with every life-cycle aspect of structural and nonstructural component [3]. The necessity of risk assessment for all types of structure subjected to high wind disaster have been highlighted in many previous researches including wind load statistic determination by Ellingwood and Tekie [4], wind fragility for industrial buildings by Ham et al. [5], and an apartment buildings' balcony window in [6]. Additionally, Lee and Rosowsky [7]

and Ellingwood [8] analyze fragility curve for a wood frame structure subject to lateral wind loads by means of the Monte Carlo Simulation (MCS) method, which is a part of analytical fragility development. That method was based on statistical wind load parameters determined by Ellingwood and Tekie [4] by means of Delphi questionnaire. Moreover, combined, the statistical parameters with wind loads standard code ASCE 7-10 [9] can be applied to a of structure types.

Wind fragility  $P_f(V)$  is defined as the conditional probability of failure when a component or system of structure attains or exceeds a specified criterion [10], as can be seen in:

$$P_f(V) = P[R - W \leq 0 | V] \quad (1)$$

where,  $R$  = resistance capacity,  $W$  = wind loads, and  $V$  = a particular wind speed at which the probability of failure is evaluated.

In this study, the development of fragility was based on analytical method by mean of the MCS method and based on resistance capacity data and statistical wind loads data, as shown in the next section. In general, the fragility function can be defined as a mathematical function of probability whose variation is generated by external excitation reached or exceeded a specified limit state. It is commonly described by lognormal distribution as [10]:

$$Fr(V) = \Phi \left[ \frac{\ln(x) - \mu_R}{\sigma_R} \right] \quad (2)$$

in which  $\Phi(\cdot)$  = standard normal cumulative distribution function,  $\mu$  = logarithmic median of resistance capacity, and  $\sigma$  = logarithmic standard deviation of resistance capacity  $R$ . By using lognormal CDF for the fragility model, which is commonly used, it can be convolved with a hazard map for any specific area to develop the risk assessment framework. This framework can be used to provide an accurate source for a hazard mitigation plan [11].

Previous studies [12], [13] were the development of wind fragility for windows components and the connection used in small-scale steel frame structures. Therefore, for better comprehending the performance of these small-scale structures during wind disaster, the determination of roof cladding components was focused on in this study. Firstly, by using Monte Carlo Simulation (MCS) method to simulate random wind loads based on the ASCE 7-10 wind loads design guidelines and wind load statistical parameters from Ellingwood and Tekie [4], the probability of failure for roof

V. Sim is with the Department of Civil Engineering, Gangneung-Wonju National University, South Korea.

W. Y. Jung, Professor / Ph.D., is with the Department of Civil Engineering, Gangneung-Wonju National University, Gangneung, South Korea (e-mail: woojung@gwnu.ac.kr).

cladding was determined. Then, by presenting the probability of failure in the form of lognormal distribution in (2), the parameters of wind fragility for roof cladding were established.

## II. DESCRIPTION OF STRUCTURE AND LOADS

The structure in this case study is a small-scale two storey steel frame structure as can be seen in Fig. 1. The focus of this study is the failure of roof cladding and their configuration, which is shown in Fig. 2. The roof of this structure is gable roof type with 18° slope. Moreover, this two storey house was considered to be representative of much of the residential buildings in Korea.

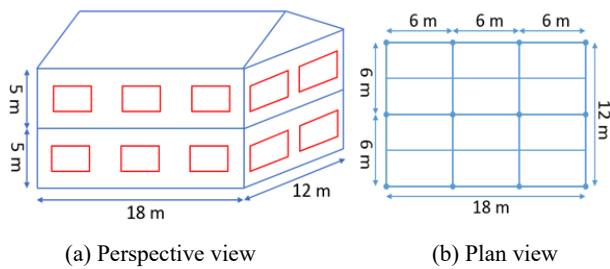


Fig. 1 Dimension of steel frame structure

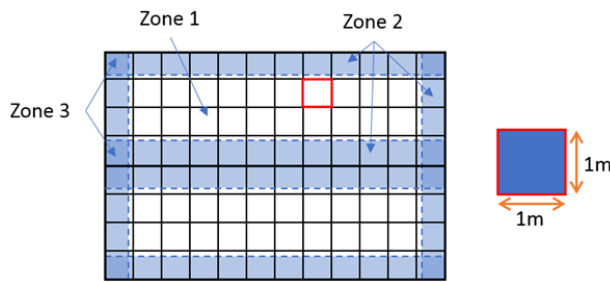


Fig. 2 Roof cladding configuration

In Fig. 2, Zone 1, Zone 2 and Zone 3 were three different wind zones with different pressure coefficients designated in ASCE 7-10. In ASCE 7-10, the wind pressure acting on the components and cladding for low-rise structures is determined as:

$$W = q_h (GC_p - GC_{pi}) \quad (\text{unit: } N/m^2) \quad (3)$$

where  $q_h$  = velocity pressure evaluated at mean roof height  $h$ ,  $GC_p$  = product of gust factor and external pressure coefficient, and  $GC_{pi}$  = product of gust factor and internal pressure coefficient. The velocity pressure calculated at height  $z$  is given by:

$$q_z = 0.613K_zK_{zt}K_dV^2 \quad (\text{unit: } N/m^2) \quad (4)$$

where  $K_z$  = the velocity pressure exposure factor,  $K_{zt}$  = the topographic factor,  $K_d$  = the wind directionality factor,  $V$  = the basic wind speed in  $m/s$ . Wind loads are considered, for the purpose of design, as distributed static loads. The gust pressure coefficient,  $GC_p$ , varies by panel location, e.g. panels located at

the edge of the roof have higher external pressures than those in the interior. From Fig. 2, effective external pressure coefficients for individual panels can be determined by using weighted average method (a sum of the external wind pressures on specific zones – e.g. zone 1, zone 2 or zone 3 – multiplied by the fraction of cladding panel area over which those pressures are assumed to act).

Furthermore, from those nominal value determined above, the corresponding random variables were determined based on information by Ellingwood and Tekie [4]. Statistical values of these wind loads parameters, Tables I and II, were used to determine the random wind loads in MCS method. By multiplying Mean-to-Nominal with the nominal value determined in ASCE 7-10, a mean value for wind loads parameters was determined; from this mean value, the standard deviation could be calculated based on Coefficient of Variation (COV). Thus, normal distribution parameters (mean and standard deviation) for  $K_z$ ,  $K_d$ ,  $GC_{pi}$  and  $GC_p$  could be used to generate random wind loads.

TABLE I  
SUMMARY OF STATISTICAL WIND LOAD PARAMETERS [10]

Parameters	Category	Mean-to-Nominal	COV	Mean ( $\mu$ )	SD ( $\sigma$ )	CDF
$K_z$	Exposure B	1.01	0.19	0.72	0.14	Normal
	Exposure C	0.96	0.14	1.00	0.13	Normal
	Exposure D	0.96	0.14	1.18	0.16	Normal
$K_d$	C & C	1.05	0.16	0.89	0.14	Normal
	Enclosed	0.83	0.33	0.15	0.05	Normal
$GC_{pi}$	Partially Enclosed	0.92	0.33	0.46	0.15	Normal
$GC_p$		see Table II				
$K_{zt}$		Deterministic (1.0)				

## III. PROBABILITY OF FAILURE FOR INDIVIDUAL ROOF PANEL

A roof system was comprised of a collection of individual cladding panel; it is required to determine the probability of failure for an individual panel. Probability of failure for each roof panels, i.e. Panel a, b and c, was determined based on (1) where MCS method was used to simulate random wind loads  $W$  at each wind speed  $V$  based on (3) and (4). A large number of random wind loads were generated, in this case 5000, then by comparing them with resistance capacity  $R$  and dead loads  $D$  of roof panels, the number of panels reached failure ( $R + D - W \leq 0$ ) was found. Thus, the probability of failure for roof panel a, roof panel b and roof panel c was obtained at the specific wind speed  $V$ . By repeating this step until total failure occurred, the fragility parameters  $\mu$  and  $\sigma$  can be attained with (2).

In Fig. 3, the fragility curve for panel a, b and c was shown. Panels in these three locations have different external pressures (see Table II). The individual panel fragility curves are used in the next section to calculate the fragility of a complete roof system.

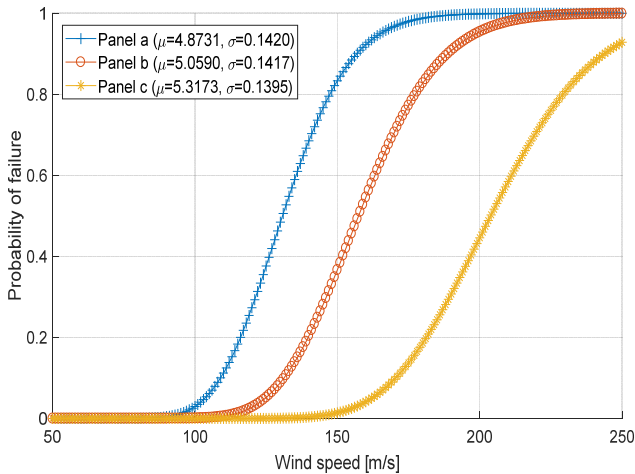


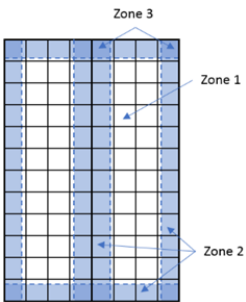
Fig. 3 Fragility curve of individual panel

TABLE II  
 SUMMARY OF  $GC_p$  STATISTIC

Nominal $GC_p$ (ASCE 7-10)			Nominal $GC_p$ at each panel		
Zone 1	Zone 2	Zone 3	Panel a	Panel b	Panel c
-0.9	-1.7	-2.6	-2.421	-1.620	-0.9
Statistical value of $GC_p$ at each panel			Panel a	Panel b	Panel c
			$\mu$	$\mu$	$\mu$
			0.28	-1.54	0.18
			$\sigma$	$\sigma$	$\sigma$
			-2.30	0.28	-0.86
			0.10		

a	b	b	a	a	b	b	a
b	c	c	b	b	c	c	b
b	c	c	b	b	c	c	b
b	c	c	b	b	c	c	b
b	c	c	b	b	c	c	b
b	c	c	b	b	c	c	b
b	c	c	b	b	c	c	b
b	c	c	b	b	c	c	b
b	c	c	b	b	c	c	b
b	c	c	b	b	c	c	b
b	c	c	b	b	c	c	b
b	c	c	b	b	c	c	b
a	b	b	a	a	b	b	a



IV. PROBABILITY OF FAILURE FOR ROOF CLADDING SYSTEM

The probability of failure of an individual roof panel was investigated in the previous section. From this result, simple reliability concepts were utilized to determine the fragility for the roof system, which consisted of the above three panel types. The limit state of this fragility was defined by the failure of multiple roof panels [3]. Three damage states correspond to the number of roof panels failure were defined as following:

- Damage state 1: number of roof panel failures  $\leq 1$  panel
- Damage state 2: number of roof panel failures  $\leq 10$  panels (10% of total panel)
- Damage state 3: number of roof panel failures  $\leq 24$  panels (25% of total panel)

In damage state 2 and damage state 3, the internal pressure condition was assumed to be fully enclosed before the failure of the first roof panel, then the condition adjust to partially enclosed for the failure of the second panel. Moreover, roof panel failures were assumed to be statistically independent even though the pressure field acting over the roof is spatially correlated and adjacent panel resistance capacities may be

correlated as a result of sharing a common roof framing. However, the assumption of independence is known to be conservative.

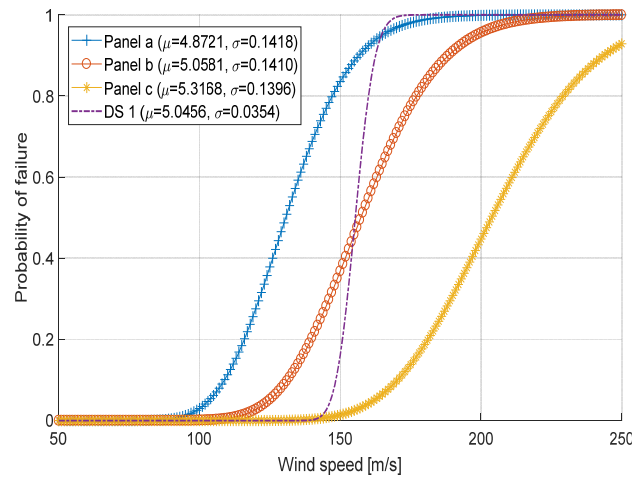


Fig. 4 Damage state 1 fragility

In Fig. 4, damage state 1 fragility was shown in purple line. The median failure occurs at 155 m/s wind speed; this means that 50% of failure would occur above wind speed 155 m/s. Additionally, to show the survivability of roof system, Fig. 5 presents the fragility of all three damage states. The curve shows that the first and second damage state have similar probability of failure. This means that just a minute increment of wind speed can increase the number of roof panel failure greatly. However, damage state 3 occurs at a much higher wind speed.

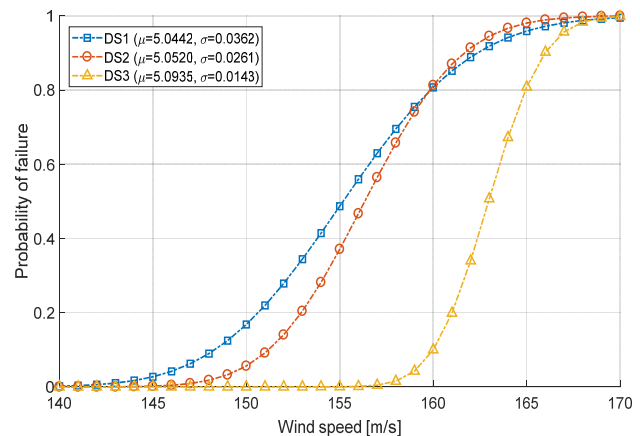


Fig. 5 Damage state 1, damage state 2 and damage state 3 fragility in exposure B

To consider the effect of building geographical location, the fragility for different exposure category was shown in Fig. 6. The exposure category is defined based on the surface roughness of the natural topography, vegetation, and constructed facilities. Exposure B is a typical residential subdivision or wooded area, Exposure C is open terrain or hurricane prone shorelines, and Exposure D is a flat and

unobstructed area within a ¼ mile of an inland lake at least one mile across. This means that Exposure D will experience a higher wind pressure, which is also reflected in Fig. 6 with a higher probability of failure at the same wind speed compared to the other two exposures.

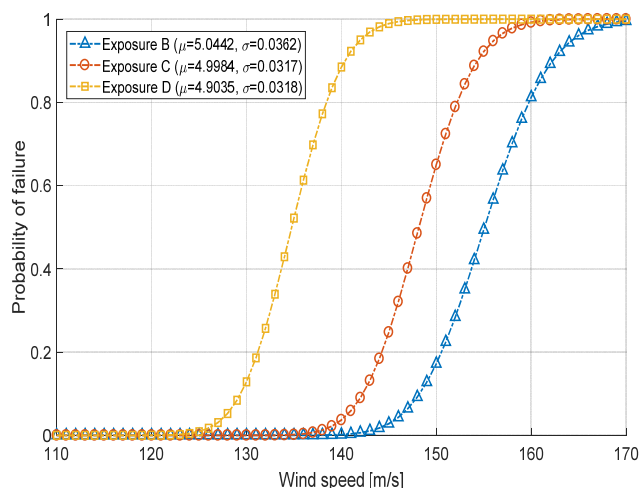


Fig. 6 Fragility for Exposure B, Exposure C and Exposure D in damage state 1

#### V. DISCUSSIONS AND CONCLUSIONS

The development of wind fragility based on Monte Carlo simulation and the experimental data of pull-out strength of screw connection was presented in this study. Moreover, lognormal CDF parameters have been used to represent these wind fragilities. These fragility parameters were determined from the probability of failure by using maximum likelihood estimation (MLE) method [14].

Results show that the failure of the panel, mostly at the edge, (Panel a) had the highest probability of failure; this is due to the high suction force of wind at the panel edge. Consequently, the probability of failure for “Panel a” had the highest value. Moreover, fragility at each damage state of the roof system was analyzed based on the system reliability concept. The shifting of the fragility curve to the right from damage state 1 to damage state 3 shows that the failure of the roof panel continuously occurs as the wind speed increases. Furthermore, the overall failure of the roof system occurs at an excessive wind speed which means the failure of this roof cladding design due to high wind is a rare occurrence. However, from the fragility parameters presented here, it can be convolved with a wind hazard map to predict the performance of roof cladding, to improve the reliability of roof system designed to resist high wind loads and to predict economic losses in an event of a high wind disaster. Further study will focus on different designs of roof systems to account for all types of small-scale structure in Korea.

#### ACKNOWLEDGMENT

This research was supported by a grant [MOIS-DP-2015-05] through the Disaster and Safety Management Institute funded

by Ministry of the Interior and Safety of Korean government.

#### REFERENCES

- [1] S. J. Chen, C. H. Yeh, and J. M. Chu, “Ductile steel beam-to-column connections for seismic resistance,” *Journal of Structural Engineering*, 1996, vol. 122, no. 11, pp. 1292-1299.
- [2] National Typhoon Center, “Typhoon White Book,” 2011, 11-1360016-000001-01.
- [3] K. H. Lee, and D. V. Rosowsky, “Fragility assessment for roof sheathing failure in high wind regions,” *Engineering Structures*, 2005, vol. 27, no. 6, pp. 857-868.
- [4] B. R. Ellingwood, and P. B. Tekie, “Wind load statistics for probability-based structural design,” *Journal of Structural Engineering*, 1999, vol. 125, no. 4, pp. 453-463.
- [5] H. Ham, S. Lee, and H. Kim, “Development of typhoon fragility for industrial buildings,” *Proceeding of the 7th Asia-Pacific Conference on Wind Engineering*, 2009.
- [6] H. J. Ham, W. Yun, H. J. Kim, and S. Lee, “Evaluation of Extreme Wind Fragility for Balcony Windows Installed in Mid/Low-Rise Apartments,” *Journal of Korean Society of Hazard Mitigation*, 2014, vol. 14, no. 1, pp. 19-26.
- [7] K. H. Lee, and D. V. Rosowsky, “Fragility curves for woodframe structures subjected to lateral wind loads,” *Wind and Structures*, 2006, vol. 9, no. 3, pp. 217-230.
- [8] B. R. Ellingwood, D. V. Rosowsky, Y. Li, and J. H. Kim, “Fragility assessment of light-frame wood construction subjected to wind and earthquake hazards,” *Journal of Structural Engineering*, 2004, vol. 130, no. 12, pp. 1921-1930.
- [9] American Society of Civil Engineers, “Minimum design loads for buildings and other structures (Vol. 7),” *American Society of Civil Engineers*, 2010.
- [10] K. Porter, “Beginner’s guide to fragility, vulnerability, and risk,” *Encyclopedia of Earthquake Engineering*, 2015, pp. 235-260.
- [11] P. J. Vickery, P. F. Skerlj, J. Lin, L. A. Twisdale Jr, M. A. Young, and F. M. Lavelle, “HAZUS-MH hurricane model methodology. II: Damage and loss estimation,” *Natural Hazards Review*, 2006, vol. 7, no. 2, pp. 94-103.
- [12] V. Sim, J. K. Choi, and W. Y. Jung, “Fragility assessment of the connection used in small-scale residential steel house subjected to lateral wind loads,” *MI-Best Conference Proceeding*, 2017.
- [13] V. Sim, Y. J. Gwak, and W. Y. Jung, “Development of wind fragility for window system in lightweight steel frame house in South Korea,” *MI-Best Conference Proceeding*, 2017.
- [14] M. Shinozuka, M. Q. Feng, J. Lee, and T. Naganuma, “Statistical analysis of fragility curves,” *Journal of engineering mechanics*, 2003, vol. 126, no. 12, pp. 1224-1231.